

Th VW 06

Use of a Robust Norm in Reducing FWI Uncertainty in the Presence of Cycle Skipping

J. Ramos-Martinez¹, A. Valenciano¹, N. Chemingui¹, T. Martin^{1*}¹PGS

Summary

Full Waveform Inversion (FWI) can create on an inaccurate model as a result of cycle skipping, if the initial model is not close enough to the true one, or there is insufficient low frequencies in the data. Furthermore, FWI model updates can be affected by a reflectivity imprint prior to the resolution of long-wavelength features. Imaging with the resulting incorrect model will create structural uncertainty, and will hamper an evaluation of potential prospects. Cycle skipping can be mitigated by using a robust norm for measuring the data misfit (W2-norm), instead of a traditional L2-norm. Used with a velocity gradient that removes the imprint of the reflectivity, we demonstrate an application to data resolving a high-velocity layer that was not present in the initial model. Corroborated by well data, the resulting earth model accurately reflects the subsurface, which, in turn, reduces uncertainty in the final structural image.

Introduction

Classic FWI (Tarantola, 1984) models can leak the reflectivity imprint into the velocity update before the long-wavelength components of the model are constructed (Mora, 1989). Practitioners follow cumbersome data selection strategies to circumvent this. Furthermore, the misfit function based on the L_2 -norm measures the difference between the recorded and modeled oscillatory signals on a point-by-point basis. Cycle skipping may occur if the starting model causes the wave simulation to be mismatched by more than half of the period of the recorded data. The inversion will converge to a wrong velocity model, leading to an image with increased uncertainty. This can be laboriously overcome, if the data permits, through a progressive combination of data selection in offset and frequency. In high contrast geological settings (e.g., salt, carbonates and volcanics), small locational errors in the reflector positioning lead to large kinematic errors. Using a different metric for the data misfit quantification is advantageous (e.g., Engquist et al., 2016; Qiu et al., 2017). We present the use of a quadratic form of the Wasserstein distance (W2-norm) to measure the data misfit with a robust implementation of the velocity gradient.

Methodology

Typically, a least-squares objective function is used for measuring the data misfit in FWI. Here we estimate the data difference using the W2-norm:

$$J = \sum_s \sum_r W_2^2(\tilde{u}, \tilde{d}) \tag{1}$$

Where $\tilde{u}(t)$ and $\tilde{d}(t)$ are encoded versions of the modeled and field data. The W2-norm and the resulting Frechet derivative are explained in Qiu et al. (2017). To produce long-wavelength updates, we adapted the equations for our velocity gradient to work with the W2 misfit function. The velocity gradient is a weighted velocity sensitivity kernel derived from the impedance and velocity parameterization of the objective function (Ramos–Martinez et al., 2016). It separates the migration isochrones produced by the specular reflectivity from the components created by transmitted arrivals. Our combined numerical implementation (Qiu et al., 2017) uses an encoding scheme based on a logistic function that assures the positiveness and mass conservation conditions required by the optimal transport theory. Ramos–Martinez et al. (2018) provided more details on the velocity gradient derivation.

Figure 1 shows the sensitivity kernels for different combinations of the L_2 -norm, W2-norm and the FWI gradients. They were computed for a source-receiver pair in a layer where velocity increases with depth. Notice that the W2 velocity kernel accentuates the long-wavelength components when compared to the L_2 -norm velocity kernels.

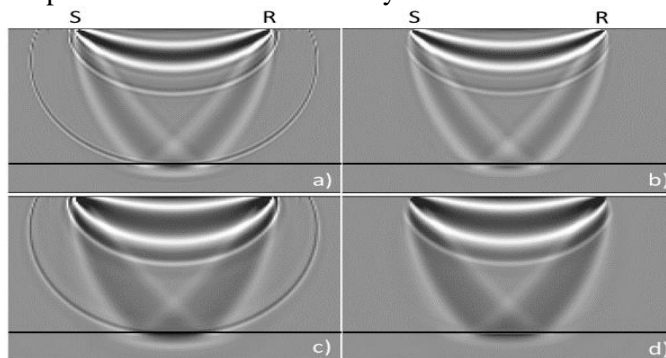


Figure 1 Sensitivity kernels of a source-receiver pair in a model with a $V(z)$ layer over a half-space for a) L_2 -norm and cross-correlation FWI gradient, b) L_2 -norm and FWI velocity gradient, c) W2-norm and cross-correlation gradient, and d) W2-norm and velocity gradient.

Example

We applied the new FWI algorithm to a field data survey acquired in the Ceará basin, offshore Fortaleza, Brazil. The acquisition comprised 14 deep tow dual-sensor streamers with a maximum inline offset of 8 km. The signal-to-noise ratio was good to 2.5 Hz; the maximum frequency used in the inversion was 8 Hz. The inversion data window contained a mix of transmitted and reflected events. The starting velocity model (Figures 2a and 3a) missed near-seafloor carbonates that create uncertainty in the seismic image as well as cycle skipping. Due to the shallow water and multiple contamination, reflection tomography updating in the near surface was limited. High contrast carbonates (~3300 m/s from a nearby well log Figure 3) limited refracted energy to 1.2 km depth.

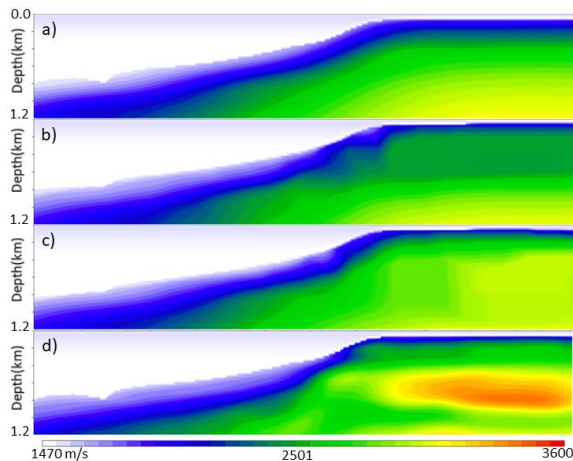


Figure 2 Model comparisons a) starting model, b) FWI - L2-norm, c) FWI - W2-norm, (d) FWI model by cascading the W2-norm and L2-norm.

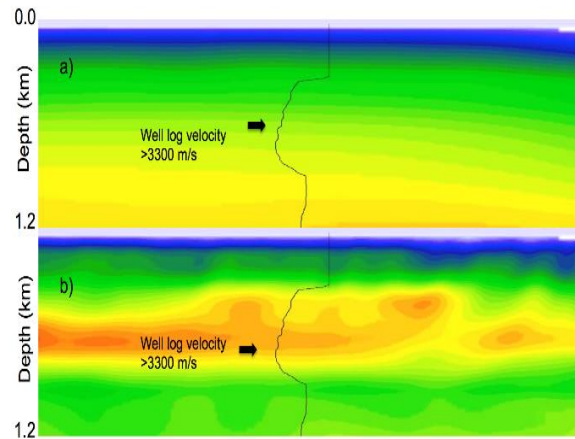


Figure 3 Model comparisons near a well: a) starting model and b) Final FWI model produced by cascading the W2-norm and L2-norm.

Figures 2b and 2c show the models initially obtained using the L2- and W2-norms; both used the velocity gradient to minimize the high-wavenumber artefacts produced by the multiples. Due to cycle skipping, the L2-norm (Figure 2b) inversion gave an update in the wrong direction, whilst the W2-norm yielded an increase in velocity where the carbonates are expected. After resolving the cycle skipping problem, we continued the inversion using L2-norm FWI (Figures 2d) to resolve the high contrast carbonates. The velocity increase was corroborated with well log data. Figure 3a and 3b show the starting and final FWI models for a line in the proximity of the well. The final FWI model matches the well trend capturing the spatial variability of the carbonates.

Conclusions

We combined a robust implementation of a velocity gradient and the optimal transport norm (W2) to solve the FWI cycle skipping problem and retrieve the long-wavelength velocity updates, reducing the dependency on accurate starting velocity models and ultra-low-frequency data. We illustrated the advantages on a field data survey where it resolved high-velocity carbonates that were missing from the starting model. Well log data corroborated the carbonates presence and validated the FWI result. The final velocity model improved the image of both shallow and deep structures.

Acknowledgements

We thank PGS MultiClient for permission to use the data, Mikhail Orlovich and Xiaoyan Jiang for the data processing, and Lingyun Qiu, Yunan Yang, Dan Whitmore, and Faqi Liu for helpful discussions.

References

- Engquist, B., Froese, B.D. and Yang, Y. [2016] Optimal transport for seismic full waveform inversion: Communications in Mathematical Sciences, **14**, 2309-2330.
- Mora, P., [1989] Inversion = migration + tomography: Geophysics, **54** (12), 1575-1586.
- Qiu, L., Ramos-Martinez, J., Valenciano, A.A., Yang Y. and Enquist, B. [2017] Full-waveform inversion with an exponentially encoded optimal-transport norm, 87th SEG Annual International Meeting, Expanded Abstracts, 1286-1290.
- Ramos-Martinez, J., Crawley, S., Zou, Z., Valenciano, A.A., Qiu, L. and Chemingui, N. [2016] A robust gradient for long wavelength FWI updates, 76th EAGE Conference & Exhibition, Extended Abstracts, Th SRS2 03.
- Ramos-Martínez, J., Qiu L., Kirkebø J., Valenciano A.A. and Yang Y. [2018] Long-wavelength FWI updates beyond cycle skipping. SEG Technical Program Expanded Abstracts 2018: pp. 1168-1172.
- Tarantola, A., [1984] Inversion of seismic reflection data in the acoustic approximation, Geophysics, **49**, 1259-1266.
- Xu, S., Wang, D., Chen, F., Zhang, Y. and Lambaré, G. [2012] Full waveform inversion for reflected seismic data, 74th EAGE Conference & Exhibition, Extended Abstracts, W024.